DAΦNE TECHNICAL NOTE

INFN - LNF, Accelerator Division

Frascati, January 27, 1996

Note: **MM-22**

THE LARGE APERTURE QUADRUPOLE PROTOTYPE FOR THE DAΦNE INTERACTION REGIONS

B. Bolli, F. Iungo, N.Ganlin, F. Losciale, M. Paris, M. Preger, C. Sanelli, F. Sardone, F. Sgamma, M. Troiani

1. INTRODUCTION

The large aperture quadrupole is a special magnet, designed to be installed near the end of the interaction region vacuum vessel, where the two beams are already well separated. In this part of the machine lattice there are special requirements both on the available aperture and on the good field region, which are much larger than in the other quadrupoles of the ring. Eight such magnets are needed in the "DAY-ONE" structure [1] used during the first commissioning of the collider, while four of them will be permanently in operation around the FINUDA [1] detector. Figures 1 and 2 show a front view of the quadrupole and its side view respectively.

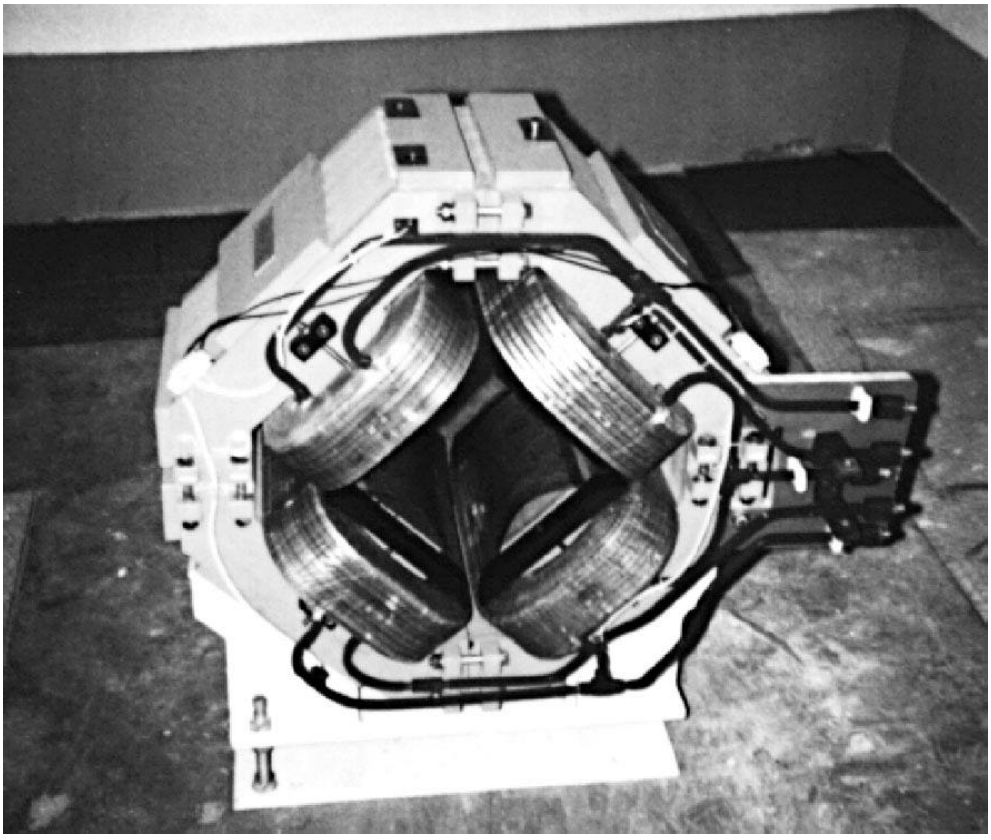

Figure 1 - Front view of the large aperture quadrupole prototype

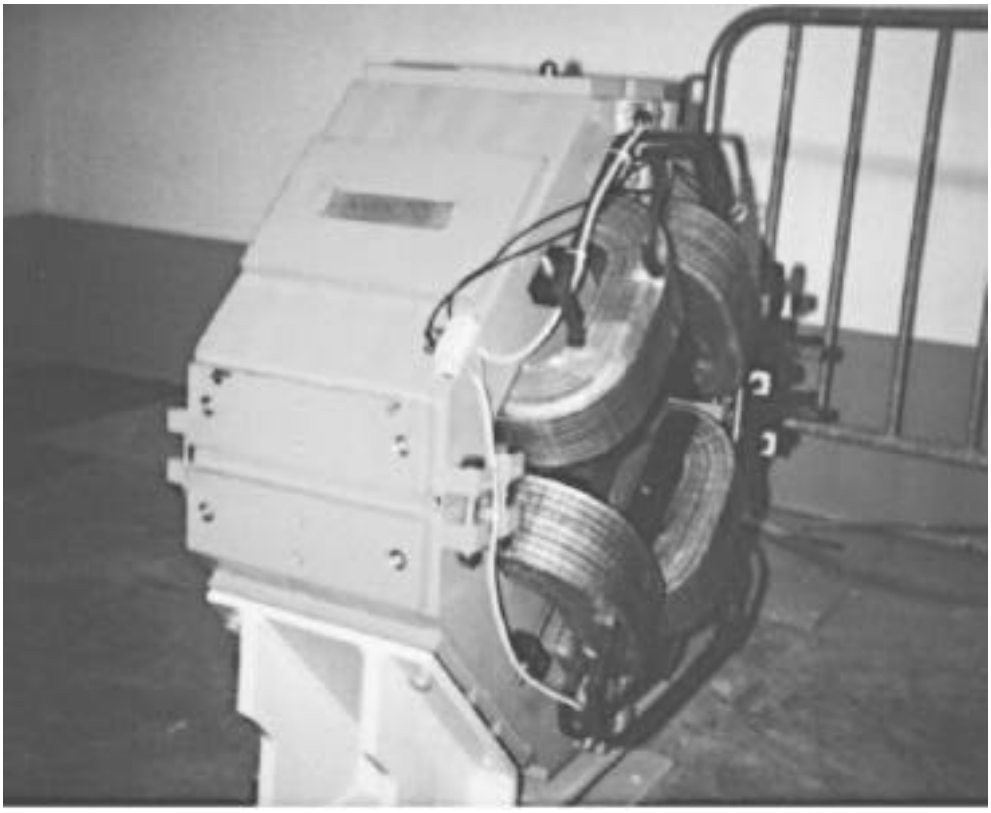

Figure 2 - Side view of the large aperture quadrupole prototype

The first prototype of the large aperture quadrupole has been delivered to LNF on November 14, 1996. It has been characterized from the electrical and magnetic points of view. Even if the field quality was not found to be within specification, the magnetic measurements have shown, as explained in detail in the following, that the leading high order component of the field error is the sextupolar one, which can be corrected by means of the lumped sextupoles in the lattice. The magnet has therefore been accepted and Ansaldo authorized to proceed to series production (7 other magnets), with the recommendation of a better control on the lamination stacking and assembling procedures.

Table I shows the latest values for the required gradients. Table II lists the main design parameters of the magnet. Table III gives the design coordinates of the pole profile, shown in Fig. 3.

Table I - Required gradients for nominal length

	K^2 (m^{-2})	Gradient @ 510 MeV (T/m)
DAY-ONE #1	2.049	3.483
DAY-ONE #2	3.753	6.380
FINUDA #1	1.326	2.254
FINUDA #2	1.990	3.383

Table II - Design parameters of the large aperture quadrupole

Quantity		8
Energy	MeV	510
Nominal gradient	T/m	6.2
Bore radius	mm	100
Good field region	mm	± 66
Field quality $\|\Delta B/B\|$		$\leq 5*10^{-4}$
Magnetic length	m	0.4
Turns per pole		54
Ampere-turns per pole	A	24830
Nominal current	A	459.8
Current density	A/mm^2	6.49
Copper conductor cross section	mm*mm	10*10
Cooling hole diameter	mm	6
Resistance per magnet @ 60 °C	mΩ	61.2
Voltage per magnet	V	28.14
Power per magnet	kW	12.94
Water circuits per magnet		4
Total water flux per magnet	L/s	0.155
Pressure drop	ATM	2.6
Water inlet temperature	°C	32
Water temperature rise	°C	20

TABLE III - Pole profile coordinates

Point	X (mm)	Y (mm)	Point	X (mm)	Y(mm)
A	70.71	70.71	B	100.00	50.00
A1	73.64	67.90	C	130.85	36.27
A2	76.57	65.30	D	147.85	36.27
A3	79.50	62.90	E	230.78	119.20
A4	82.43	60.66	F	282.00	67.98
A5	85.35	58.58	G	282.00	0.00
A6	88.28	56.64	H	377.00	0.00
A7	91.21	54.82	I	377.00	107.36
A8	94.14	53.11	L	242.18	242.18
A9	97.07	51.51			

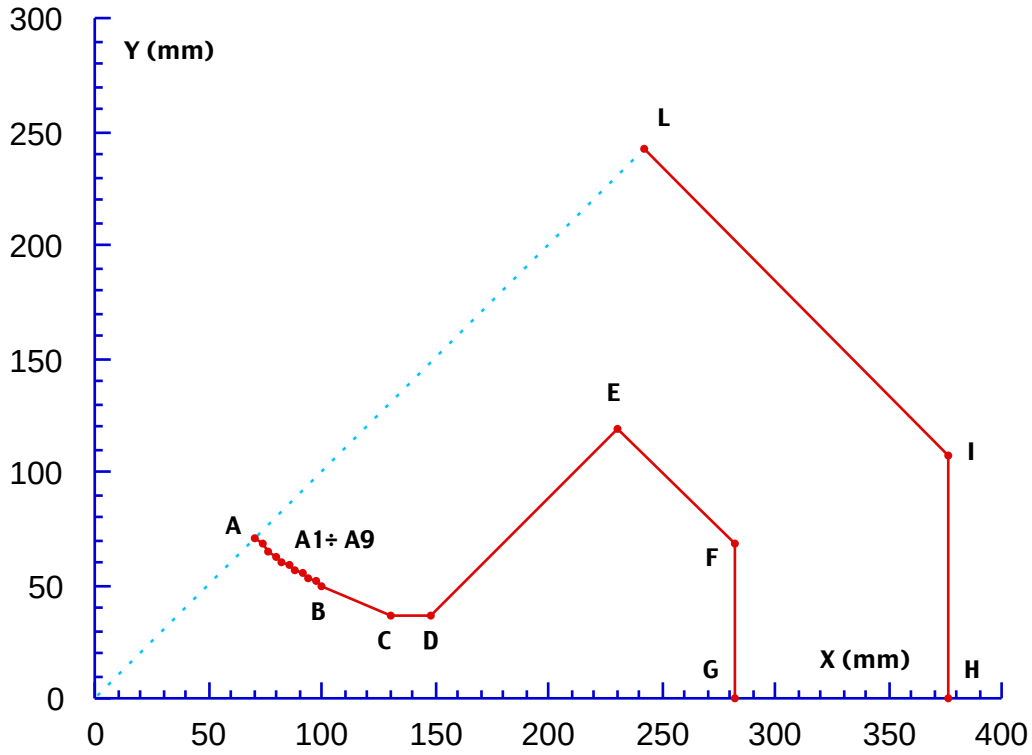

Figure 3 - Lamination profile

2. ELECTRICAL MEASUREMENTS

The resistance of the large aperture quadrupole prototype coils was measured by means of a micro-ohm-meter (AOIP mod. OM 20) at room temperature. The measured value was:

R= 64.4 mΩ @ 23 °C

The same measurement was accomplished by using the Volt-Ampere method and the following data was measured:

V= 35.8 V @ 534 A, corresponding to 67 mΩ at an average temperature of 30 °C.

The agreement between the results obtained with the two different methods is very good.

The inductance and resistance of the magnet prototype were also measured by means of a LCR meter (LCR meter HP 4284 A) at different frequencies. The results are very similar and they are shown in Figure 4. The corresponding dc values can be extrapolated from these data. They are consistent with the measured and design data.

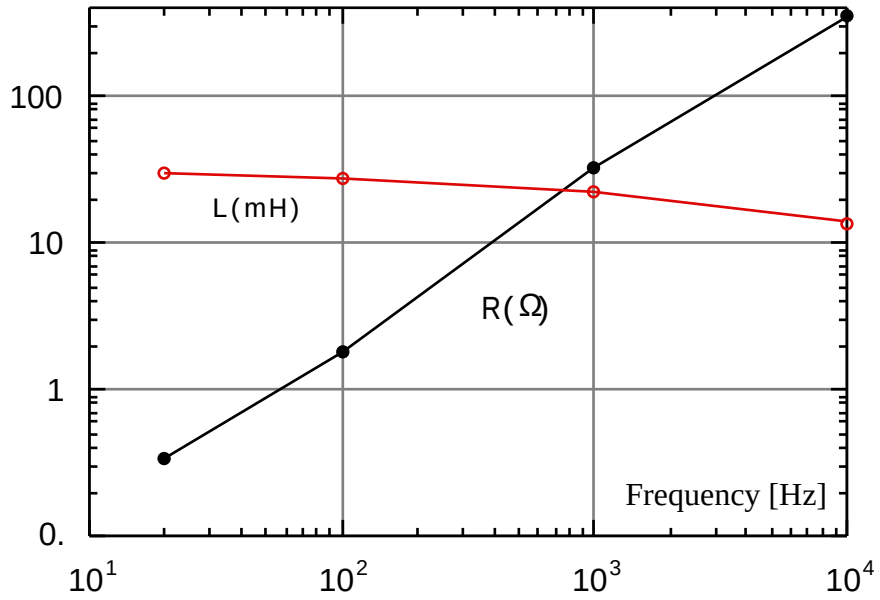

Figure 4 - Resistance and inductance versus frequency

Thermal measurements were also accomplished and the worst figure for the quadrupole magnet is listed in Table IV.

Table IV - Temperature rise of magnet coils.

Time (min)	0	1	2	3	4	5	6
Temperature (°C)	18.5	26.5	36.1	41.5	43.2	443.5	43.7

3. MAGNETIC MEASUREMENTS

A first set of measurements with the Hall probe positioning system [2] has been performed in order to check the current values necessary to reach the integrated gradient corresponding to those quoted in Table I. Figure 5 shows the gradient at the quadrupole center as a function of the excitation current. The gradient is found by measuring the vertical field component on the horizontal symmetry plane of the magnet in two points at ±30 mm from the longitudinal axis.

The vertical field component has been also measured on the longitudinal axis and along straight lines parallel to it in order to have an indication on the magnetic length before the chamfering procedure. The field has been measured in steps of 10 mm varying the distance from the symmetry axis up to ±50 mm from the center. The result is given in Fig. 6, where both the magnetic length, defined as the field integral divided by the maximum field value and the full width at half maximum are shown.

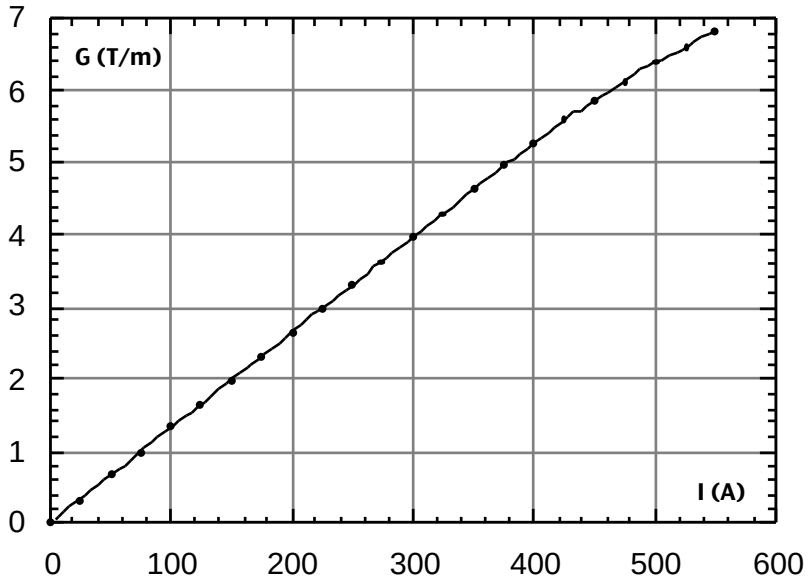

Figure 5 - Gradient at magnet center before chamfer

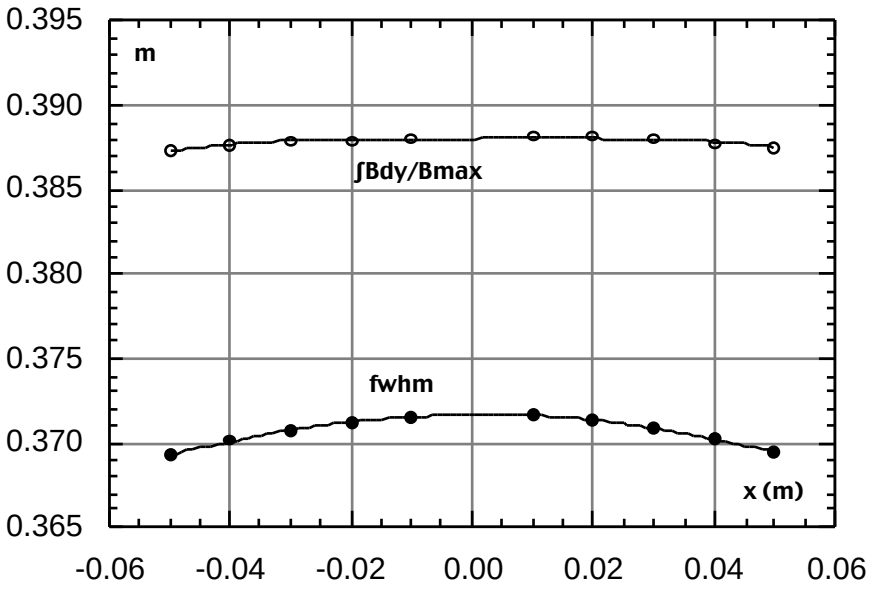

Figure 6 - Magnetic length of the large aperture quadrupole before chamfer @ 534A.

The gradients given in Table I are referred to the nominal magnetic length of 40 cm. The result of the measurements shown in Fig. 6 indicate that, in order to reach the required integrated gradients it is necessary to increase the gradients given in the Table by ≈ 3%. Combining this figure with the excitation curve in Fig. 5 we find a maximum operating current of ≈ 520A @ 510 MeV.

From the same measured map used to find the magnetic length it is possible to extract the coefficients of the transverse field expansion, following the procedure described in detail in [3], and extensively applied for the DAΦNE dipole magnets to correct the sextupole contribution of the fringing fields by means of suitable shimming techniques.

It is particularly interesting to compare the behaviour of the 12-pole component before and after chamfering the removable end caps. For this reason we show in Fig. 7 the longitudinal dependence of the fifth order term of the transverse expansion:

$$B_Z(x) = b_O + b_1*x + b_2*x^2 + b_3*x^3 + b_4*x^4 + b_5*x^5 + ...$$

The curve in Fig. 6 is not very smooth, the reason being that the measurement have not been performed far enough from the center, resulting in a reduced sensitivity to the high order terms. It is possible, however, to notice that there is a large positive contribution to the 12-pole component coming from the fringe fields, while the contribution from the central part of the magnet is very small. It was therefore easy to predict that the chamfering procedure performed on the removable end caps would be efficient.

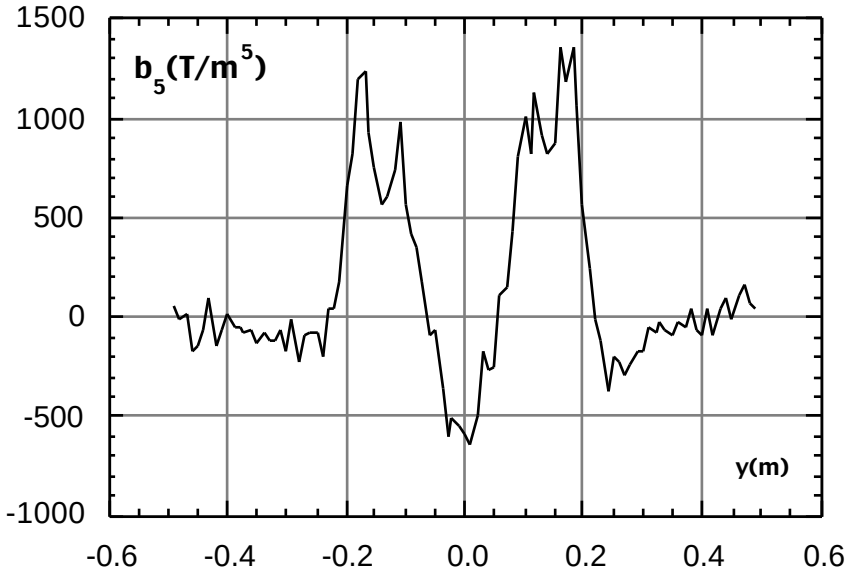

Figure 7 - Longitudinal behaviour of the fifth order term
of the transverse expansion before chamfer.

The prototype has been then placed on the rotating coil system [2] and the high order integrated field components measured as a function of the excitation current. As expected, the leading term of the field deviation from the ideal quadrupole field has been found to be the 12-pole one. Figure 8 shows the contributions of the high order terms (up to the 20-pole) for several excitation current. The contributions are extrapolated to the good field region boundary set in the Specification (66 mm), although the magnet has been measured with the same coil used for the Accumulator quadrupoles [4] and the achromat quadrupoles of the Main Rings [5], where the bore radius is half of the large aperture quadrupole one.

Of course, the best sensitivity to the high order terms is obtained when the measuring coil radius is as close as possible to the quadrupole one, which was the case for the other two kinds of quadrupoles (49 cm coil radius versus 50 cm quadrupole bore radius). For this reason, we have found that the noise contribution in the measurement of the large aperture quadrupole was unacceptably large for the high order terms above the 20-pole. Even the 20-pole, which is a systematic aberration for the quadrupoles, showed up to be at the limit of reliability, exhibiting unreasonable fluctuations between the measurements at different excitation currents and even when repeating the same measurements many times. However, we have included the 20-pole contribution into the plots, with the warning that it should be considered only as an order of magnitude estimate.

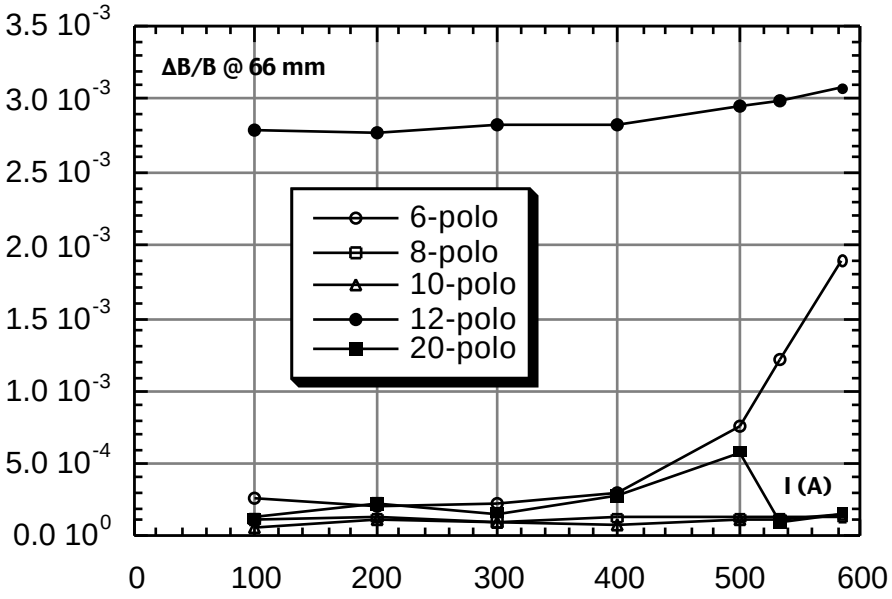

Figure 8 - Integrated high order terms @ 66 mm from magnet axis before chamfer.

In order to cancel the leading 12-pole aberration, we have followed the same procedure adopted for the Accumulator and Main Rings achromat quadrupoles [4,5], namely making a 45° cut of increasing depth on the removable end caps of the poles. Already after the first 5 mm cut it was realized that the thickness of the removable end cap (14 mm) could be not enough to cancel the 12-pole contribution. However, we proceeded first to a 10 mm cut, and then to the maximum one of 14 mm. As it can be seen from Fig. 9, where we plot the 12-pole contribution versus the cut depth on the end cap, we were left with a residual contribution ranging from 5.7×10^{-4} @ 300A to 8×10^{-4} @ 534A.

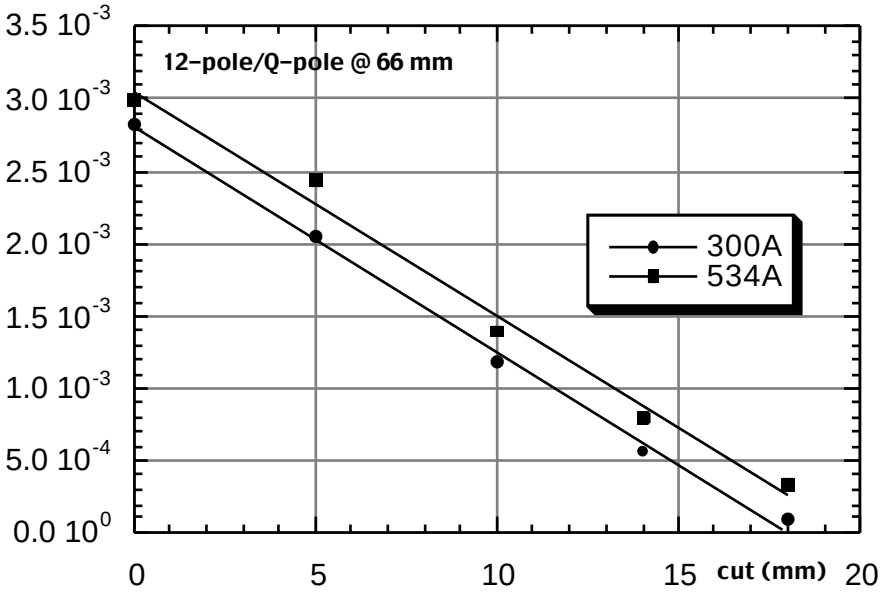

Figure 9 - 12-pole contribution @ 66 mm from magnet axis versus chamfer depth.

Being the thickness of the iron end plate 20 mm, we have therefore considered the possibility of extending the chamfer to an extrapolated value of 18 mm. We have checked the compatibility of such a cut with the mechanical characteristics of the magnet and with the manufacturer (ANSALDO) that they could machine directly the end plates before assembling the magnet. After a positive answer to both these questions, the magnet was completely disassembled, each quadrant placed as a whole on a milling machine and the final 18 mm cut performed. The magnet was then reassembled and measured again, reaching an almost perfect cancellation of the 12-pole contribution @ 300A, while the residual contribution at the maximum operating current (≈ $3x10^{-4}$ @ 66 mm) is still within the specified field quality of $5x10^{-4}$.

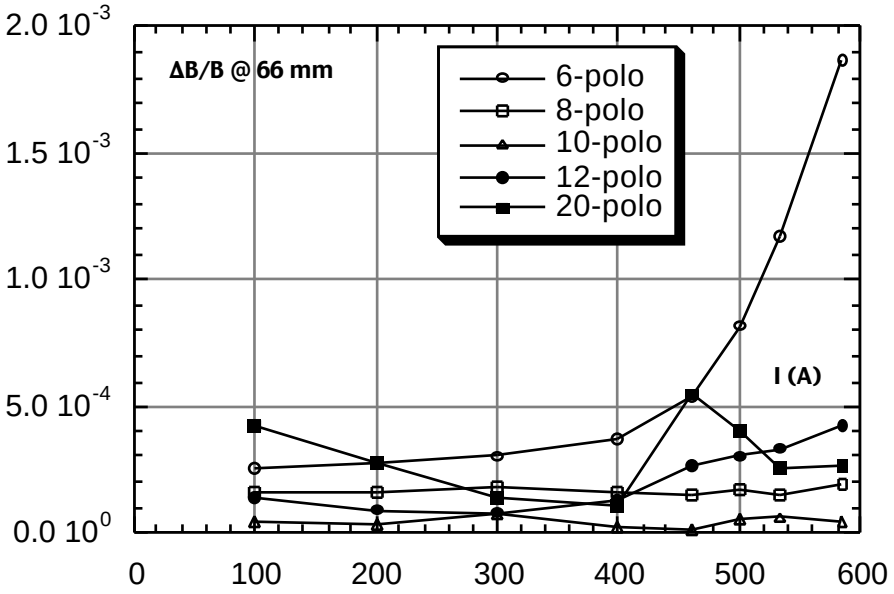

Figure 10 - Integrated high order terms @ 66 mm from magnet axis after chamfer.

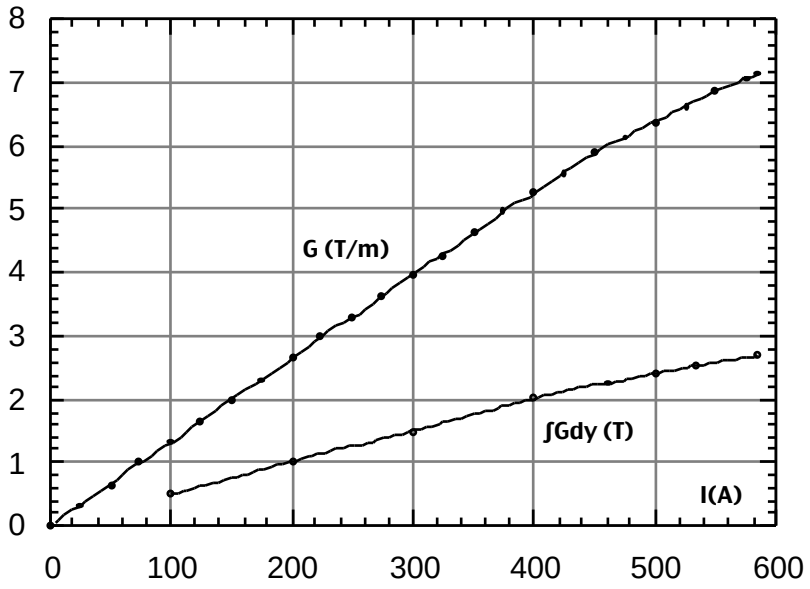

Figure 11 - Gradient at magnet center and integrated gradient after chamfer

Figure 10 shows the contribution of the most important high order terms with the final chamfer. Having corrected the 12-pole contribution, we are left with a sextupole component exceeding the Specification limit above 450 A, and with a 20-pole, which, reminding the above mentioned warnings, reaches the limit @ 100 A and 460 A. The steep increase of the sextupole component at high current is probably coming from a non perfect match of the quadrants, but it is always possible to compensate this small contribution to the overall machine chromaticity with the lumped sextupoles in the lattice. Figure 11 shows the integrated gradient, measured with the rotating coil system, together with the gradient measured at the magnet center with the Hall probe system after the chamfering procedure.

After the final measurements with the rotating coil, the magnet has been measured again with the Hall probe system to find the magnetic length after the chamfering procedure. The vertical field component has been measured, like before chamfering, along straight lines parallel to the magnet axis, but this time the measurements have been extended up to 70 mm from the magnet center. Figure 12 shows the measured field versus the longitudinal position at different distances from the axis. The measurements have been performed at two excitation currents, 300A and 534A.

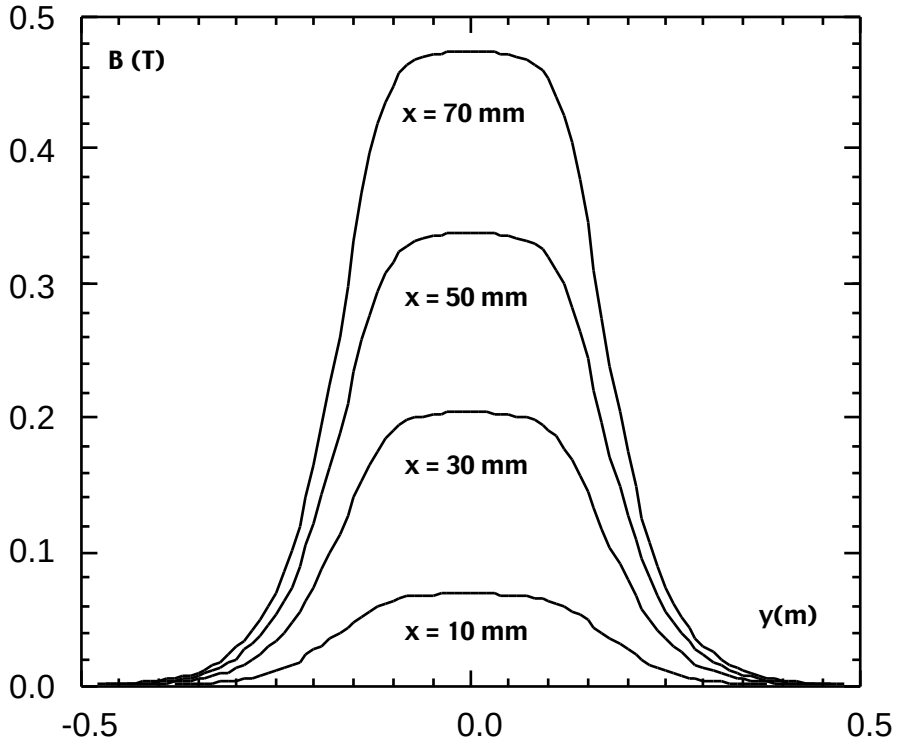

Figure 12 - Vertical field component on the horizontal symmetry plane versus longitudinal position at different distances from the magnet axis (I = 534A)

The magnetic length, defined as the field integral along one of the straight lines parallel to the magnet axis divided by the maximum measured field and the full width at half maximum are shown for both currents in Fig. 13 as a function of the horizontal distance from the magnet axis. The reduction in magnetic length due to the end cap chamfering is ≈10mm.

From the measured field maps we have considered again the transverse expansions, and it is interesting to compare the longitudinal behaviour of the 12-pole term after chamfer, shown in Fig.14 with that given in Fig. 7, representing the same quantity before chamfer. The 45° cut on the end caps introduces a negative peak in the fringing field, which compensates the large original positive peaks. Looking at the absolute values of the peaks, it is clear that there is a cancellation in the integral, but the fifth order term itself oscillates rapidly within the magnetic length of the quadrupole.

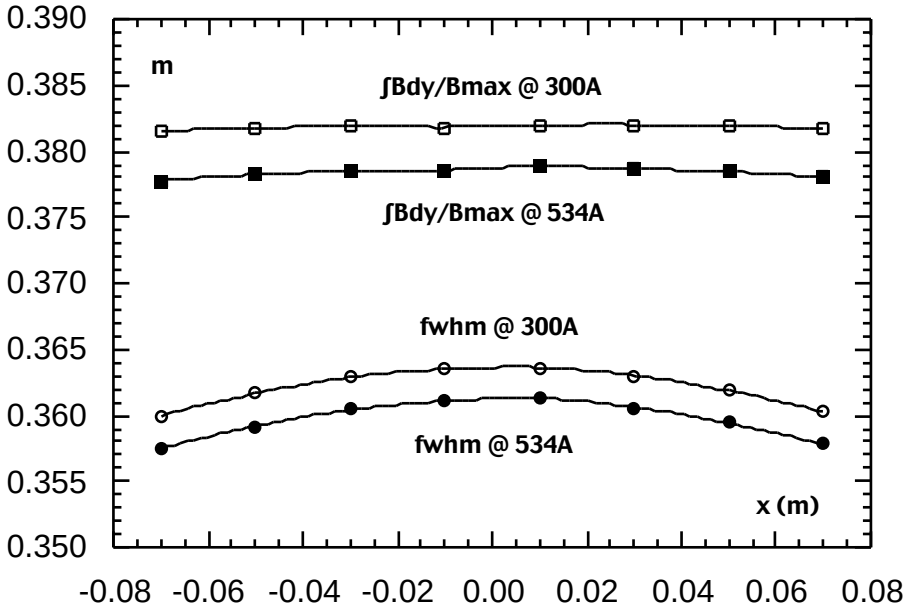

Figure 13 - Magnetic length of the large aperture quadrupole after chamfer

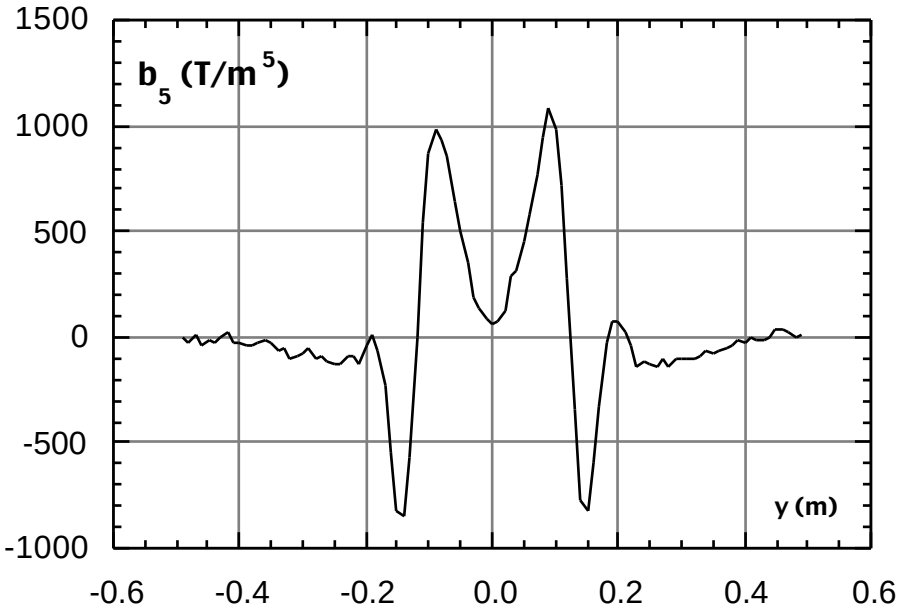

Figure 14 - Longitudinal behaviour of the fifth order term
of the transverse expansion after chamfer (I = 534A)

For sake of completeness, we show in Figs.15, 16 and 17 the longitudinal behaviour of the other terms in the transverse expansion.

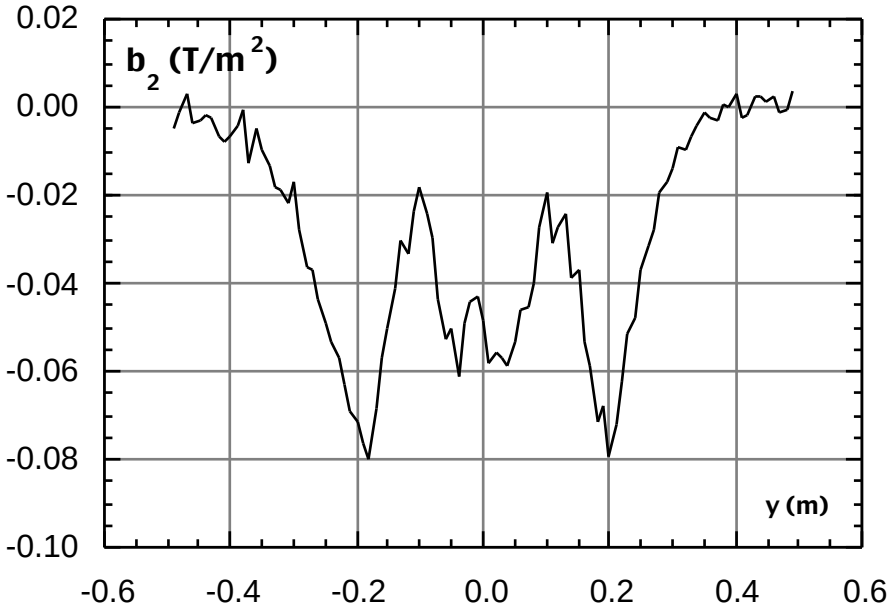

Figure 15 - Longitudinal behaviour of the second order term of the transverse expansion after chamfer (I = 534A)

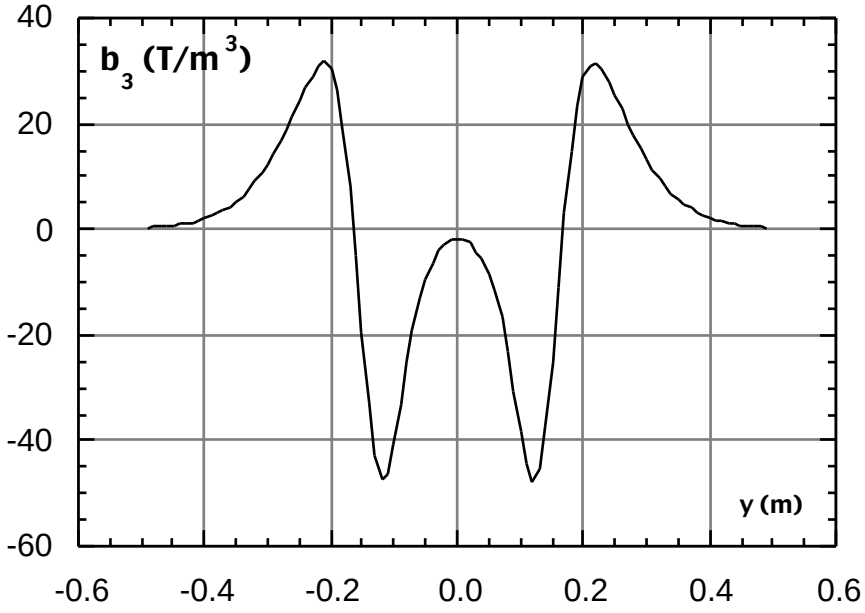

Figure 16 - Longitudinal behaviour of the third order term of the transverse expansion after chamfer (I = 534A)

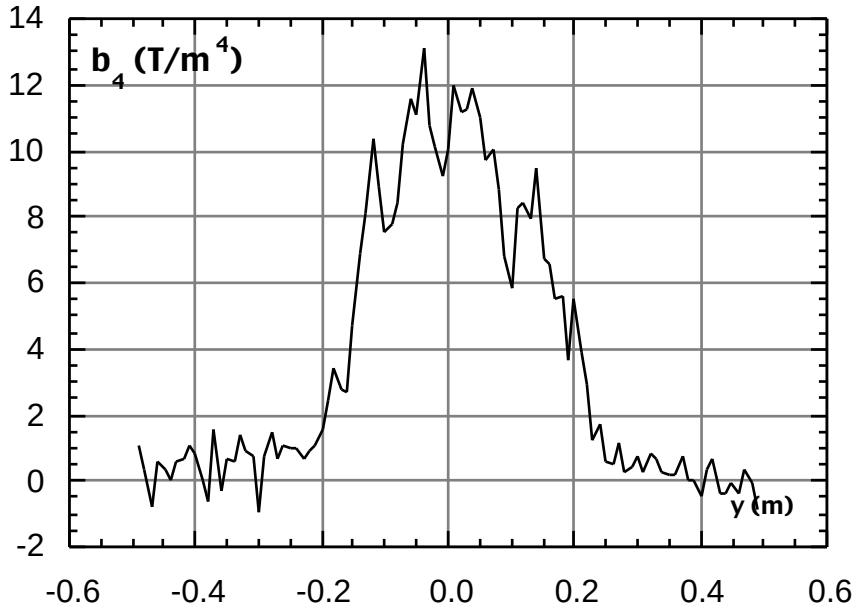

Figure 17 - Longitudinal behaviour of the fourth order term of the transverse expansion after chamfer (I = 534A)

4. CONCLUSIONS

Having the chamfer of the pole nearly cancelled the 12-pole term and relying on the possibility of compensating the 6-pole term by means of the lumped sextupoles in the rings, the quadrupole was accepted, recommending ANSALDO to realize the best coupling among the magnet quadrants during the assembling of the series magnets. The authorization for the series production was released on December 11, 1996 and the delivery of the other 7 magnets is expected at the end of February 1997.

REFERENCES

[1] M.E. Biagini, C. Biscari, S. Guiducci - "DAΦNE Main Rings Lattice Update" - DAΦNE Technical Note L-22 (18/3/96).

[2] F. Iungo, M. Modena, Q. Qiao, C. Sanelli - "DAΦNE magnetic measurements systems" DAΦNE Technical Note MM-4 (2/12/94).

[3] A. Battisti, B. Bolli, F. Iungo, F. Losciale, M. Paris, M. Preger, C. Sanelli, F. Sardone, F. Sgamma, M. Troiani, S. Vescovi - "Measurement and tuning of the DAΦNE Accumulator dipoles" - DAΦNE Technical Note MM-9 (29/8/95).

[4] B. Bolli, F. Iungo, M. Modena, M. Preger, C. Sanelli, F. Sardone, F. Sgamma, M. Troiani, S. Vescovi - "Measurements on TESLA quadrupole prototype for the DAΦNE Accumulator and Main Rings" - DAΦNE Technical Note MM-4 (2/12/94).

[5] B. Bolli, F. Iungo, N. Ganlin, F. Losciale, M. Paris, M. Preger, C. Sanelli, F. Sardone, F. Sgamma, M. Troiani, - "Misura delle caratteristiche magnetiche del quadrupolo prototipo per gli archi dei Main Rings" - DAΦNE Technical Note MM-13 (19/4/96).